Optogenetic excitation and inhibition of the subthalamic nucleus (STN) induce opposite motor effects

Adriane Guillaumin[1], Msc, Gian Pietro Serra[1], PhD,

François Georges[2], PhD, Åsa Wallén-Mackenzie[1], PhD*

[1] Department of Organism Biology, Uppsala University, SE-752 36 Uppsala, Sweden

[2] Neurodegenerative Diseases Institute, University of Bordeaux, FR-33000 Bordeaux, France

* Communicating author: Åsa Wallén-Mackenzie, E-mail: asa.mackenzie@ebc.uu.se

Word count: 3685 (excluding abstract, figure legends, references)

Key words: basal ganglia, deep brain stimulation, locomotion, optogenetics, subthalamic nucleus

Financial Disclosure/Conflict of Interest: All authors declare no actual or potential competing financial interests related to research covered in this article that might reasonably be perceived as relevant. All authors declare no conflict of interests.

Funding sources for study: This work was supported by Uppsala University and by grants to Å.W.M from the Swedish Research Council (SMRC 2017-02039), the Swedish Brain Foundation (Hjärnfonden), Parkinsonfonden, and the Research Foundations of Bertil Hållsten, Zoologiska and Åhlén.

Abstract

Background: The subthalamic nucleus (STN) is a major regulator of intended movements. The STN is controlled by both excitatory and inhibitory inputs. Dysregulation of the STN contributes to motor deficiency in Parkinson´s disease (PD). Both STN-lesioning and high-frequency electrical stimulation of the STN improve motor symptoms in PD.

However, despite a pivotal clinical target, the natural role of the STN in motor regulation has remained elusive. In fact, controlled excitatory or inhibitory manipulations have been poorly explored. By controlled regulation, new functional knowledge of the STN can be reached.

Objective: To uncover the role of the STN in several aspects of motor function during non-pathological conditions.

Methods: The Pitx2-Cre mouse model has been described as a transgenic tool to direct genetic targeting events to the STN. Here, Pitx2-Cre mice were used to direct optogenetic excitation and inhibition to the STN. The impact of each type of stimulation on motor output was recorded and compared.

Results: Optogenetic excitation of the STN triggered action potentials in a key component of the basal ganglia. Optogenetic excitation of the STN in the freely-moving animal reduced vertical and horizontal movement, induced immediate grooming and caused loss of motor coordination. In contrast, optogenetic inhibition increased general locomotion and reduced natural grooming. Opposite rotations were observed upon unilateral excitation and inhibition of the STN.

Conclusions: Optogenetic excitation and inhibition of the STN give rise to opposite motor responses in several parameters relevant to voluntary motor control that are commonly disturbed in PD.

Introduction

Basal ganglia pathways are crucial for regulation of movement. Via the direct pathway, intended movements are promoted while via the indirect and hyperdirect pathways, competing motor programs are suppressed and stop signals mediated [1–3]. A key component of both the indirect and hyperdirect pathways is the subthalamic nucleus (STN). The excitatory nature of the STN allows it to counteract the direct pathway through opposite action on the main basal ganglia output structures, the globus pallidus *interna* (GPi) and substantia nigra *pars reticulata* (SNr) [4–6].

The activational level of the STN thus serves as a critical gate of motor output, and is carefully regulated by both excitatory and inhibitory inputs. Inhibitory control is derived primarily from the globus pallidus *externa* (GPe), and excitatory control from the cerebral cortex and thalamus, and the STN is also in reciprocal connection with the GPe [7–11]. Given its gating role in motor control, dysregulation of the STN activity is strongly associated with both hypo- and hyperkinesia. Excessive activity of the STN has been correlated with the hypokinetic symptomology of PD, while unilateral damage to the STN causes hyperkinesia in hemiballismus [12].
Confirming the critical impact of the STN, PD motor symptoms can be improved by STN surgery, either by lesioning, so called subthalamotomy, or by insertion of electrodes to achieve electrical stimulation of the subthalamic area, so called deep brain stimulation (DBS) [13,14]. STN-DBS shows outstanding track record in alleviation of motor symptoms [15,16]. However, some patients suffer adverse side-effects, and neurocircuitry mechanisms upon clinical intervention of STN activity have remained elusive [17,18]. Improved knowledge of the neurobiological underpinnings of motor control exerted by the STN should help improving predictability and usability of STN-based treatments.

Optogenetics allows spatially and temporally precise control of neural activity in experimental animals [19]. Application of optogenetics in rodent parkinsonian models have shown that optogenetic excitation of cortico-subthalamic fibers in the hyperdirect pathway improves motor symptoms while its inhibition worsened them [10,11,20]. Recently, optogenetic STN-DBS verified the contribution of the STN structure in mediating beneficial effects on motor dysfunction [21]. While the use of optogenetics in parkinsonian models have thus begun to answer fundamental questions around STN-DBS mechanisms, the natural role of the STN as a gate in motor control has been poorly explored. To further knowledge, we reasoned that controlled optogenetic manipulation of excitatory *vs* inhibitory stimulation of the STN structure would be a valuable approach to unravel its contribution to complex motor functions. Optogenetics-based excitatory *vs* inhibitory analysis have recently contributed

advanced knowledge of the roles of the striatum and GP in motor output [22,23], but is still missing for the STN. A complete picture of the functional contribution of each brain structure involved in regulating motor output during normal conditions is crucial to improve clinical interventions in motor disorders.

In this study, we aimed to tease out the impact of the STN on several movement parameters during non-pathological conditions. Based on our previous work validating optogenetic excitation of the STN using Pitx2-Cre mice to achieve selectivity [24,25], protocols were here designed to allow direct comparison of the impact of optogenetic STN excitation and inhibition on motor output. Results now show that optogenetic excitation and inhibition gives rise to distinct mirror effects in several different motor parameters: STN inhibition enhances locomotion and reduces grooming; STN excitation reduces locomotion and induces grooming; STN excitation reduces balance and coordination. These findings contribute to increased understanding of motor control.

Results

Expression of optogenetic constructs in the STN of Pitx2-Cre mice with c-Fos induced upon photoexcitation confirms experimental setup

The *Pitx2* gene encodes a transcription factor essential for STN development and function [26–28]. We recently verified that expression of the optogenetic ion channel Channelrhodopsin (ChR2) in the STN of Pitx2-Cre mice causes post-synaptic currents and glutamate release in STN target areas upon photostimulation [24,25], thus validating the use of optogenetics in Pitx2-Cre mice for the study of STN.

Here, to allow excitatory and inhibitory control of STN neurons, Pitx2-Cre mice were bilaterally injected with an adeno-associated virus (AAV2) containing a DNA-construct encoding either the excitatory ion channel hChR2 (Pitx2/ChR2 mice) or the inhibitory proton pump Archaerhodopsin eArch3.0 (Pitx2/Arch mice), both opsin constructs fused with the enhanced yellow fluorescent protein, eYFP (Figure 1A). As controls, separate cohorts of Pitx2-Cre mice were injected with AAV2 expressing the fluorescent reporter eYFP alone (same control virus but different cohorts of mice, thus referred to as Pitx2/eYFP-C mice for the controls to Pitx2/ChR2 mice; Pitx2/eYFP-A for the controls to Pitx2/Arch mice). In all mice, optical cannulas were placed above the STN allowing for photostimulation at 473 nm for Pitx2/ChR2 mice and 532 nm for Pitx2/Arch mice (Figure 1A).

Different cohorts of mice were used for electrophysiological recordings and behavioral analyses, respectively (experimental outline, Figure 1A; statistical analysis, Supplementary

Table 1). Prior to sacrifice, behavioral Pitx2/ChR2 and Pitx2/eYFP-C mice underwent prolonged photostimulation and brains were dissected for histological validation of c-Fos, an indicator of induced neuronal activity. Upon completed functional analyses, all mice were analyzed histologically. Reporter expression, injection site and cannula placement were validated. Mice that displayed strong cellular eYFP labeling throughout the extent of the STN and optical cannulas placed immediately above the STN were included in the statistical analyses.

Histological analysis of eYFP fluorescence in the STN and projection target areas (Figure 1B) verified the selectivity of eYFP labeling in the STN structure over surrounding structures (Figure 1C-D). The entire extent of the STN was labeled, and within STN neurons, eYFP was detected throughout the cell body. No eYFP was detected in adjacently located structures, apart from weakly labeled fibers in the para-STN. Strong YFP labeling was identified in projections reaching the ventral pallidum, entopeduncular nucleus (EP, corresponding to GPi in primates), GP (GPe in primates), SNr and SN *pars compacta* (SNc) (Figure 1E-H). Further, Pitx2/ChR2 mice that had received photostimulation showed robust c-Fos labeling in the STN (Figure 1I-I') while no c-Fos labeling was detected in mice not stimulated (Figure 1J-J') or in Pitx2/eYFP-C control, even upon photostimulation (Figure 1K-K'). Thus, the STN and its target areas express the optogenetic constructs and allow neuronal activation upon photostimulation.

Optogenetic activation excites STN neurons and induces post-synaptic responses

To ensure firing and assess connectivity upon optogenetic activation of the STN, Pitx2/ChR2 mice were analyzed in two electrophysiological paradigms. Light-evoked responses of both the STN itself and one of its main target areas in motor control, the GP, were studied by *in vivo* single cell electrophysiological recordings upon optogenetic stimulation of the STN. First, an optotagging protocol (Figure 2A) was used to stimulate and record within the STN. To observe the reaction of STN neurons to photostimulation, peri-stimulus time histograms (PSTH protocol, 0.5 Hz, 5 ms bin width, 5-8 mW) were created by applying a 0.5 Hz stimulation protocol for at least 100 seconds. Action potentials in ChR2-positive STN cells were successfully evoked by STN photostimulation (Figure 2B).

Next, recordings were performed within the GP structure upon two different stimulation paradigms applied in the STN (Figure 2C). Firstly, the PSTH protocol was implemented which evoked action potentials in the majority of the recorded GP neurons (Figure 2D-F). This finding verified functional connectivity between the STN and GP. Next, based on previous confirmation of glutamate release upon optogenetic excitation [25], a photostimulation protocol designed to drive STN excitation in freely-moving animals was tested (Behavior

protocol, 20 Hz, 5 ms pulses, 5-8 mW; 100 seconds). Recordings in the GP identified increased frequency and firing rate of GP neurons for the whole duration of the stimulation, after which they returned to normal (Figure 2G-H). This finding validated post-synaptic activity in the GP upon application of the protocol intended for use in upcoming behavior analyses.

Pontamine sky blue staining confirmed the positioning of the recording electrodes within the GP structure and showed that all responding GP neurons were distributed in the central/medial aspect of the GP structure (Figure 2I-J). Quantification showed that 45% of the recorded neurons responded with excitation to both the PSTH protocol and the Behavior protocol while 20% responded to only one of the protocols and the remaining 35% did not respond at all (Figure 2J). Due to the low spontaneous activity of STN neurons, similar recordings were not performed to verify the inhibitory effect of Arch3.0. Having confirmed optogenetics-driven excitation of STN neurons and their post-synaptic responses, behavioral motor effects upon optogenetic STN activation and inhibition were next assessed.

Optogenetic excitation and inhibition of the STN induce opposite effects on both horizontal and vertical locomotion

First, Pitx2/ChR2 and Pitx2/Arch mice and their respective controls were analyzed in the open field test, allowing a qualitative and quantitative measurement of motor activity. The open field test also allows analysis of additional functions such as exploration, fear and anxiety. Mice were allowed to explore the apparatus for 5 minutes before starting the experimental protocol. This habituation period serves to avoid effects due to separation stress and agoraphobia which can induce thigmotaxis. Following habituation, mice were tested in a single 20 minute session composed of four alternating photostimulation-off (OFF) and photostimulation-on (ON) epochs (OFF-ON-OFF-ON).

During OFF epochs, primarily horizontal and vertical movements were observed, with short periods of grooming. To address motor effects upon STN excitation, the photoexcitation paradigm called Behavior protocol was applied. In response to STN photostimulation (ON), Pitx2/ChR2 mice responded with a significant reduction in vertical activity, known as rearing (Figure 3A). Also horizontal activity, measured as distance moved, speed and time spent moving was decreased upon STN-photostimulation (Figure 3B-D). By decreasing these motor parameters upon optogenetic activation of the STN (ON compared to OFF), the expected role of STN excitation in suppressing locomotion could be verified experimentally.

The time spent exploring the center of the arena, a measure of anxiety, was not affected by the stimulation (Figure 3E), but the number of exploratory visits to the center was significantly lower during ON epochs (Figure 3F). In addition, some Pitx2/ChR2 mice displayed abnormal

gait upon photoexcitation, characterized by slithering on the floor or backwards movements as indication of a lack of balance, while some showed a prominent jumping behavior (Figure 3H).

Contrary to STN activation in Pitx2/ChR2 mice, but in accordance with the anticipated role of the STN in motor control, continuous optogenetic STN inhibition in Pitx2/Arch mice resulted in increased horizontal and vertical movement (Figure 3I-L). In contrast to STN activation in Pitx2/ChR2 mice, while not affecting the time spent exploring the center (Figure 3M), STN inhibition increased exploratory activity, visible by a higher number of visits to the center during ON epochs (Figure 3N).

Further pin-pointing the opposite effects on motor parameters by STN excitation *vs* inhibition, also grooming behavior was altered in opposite directions by the optogenetic manipulations. Excitation of the STN induced significant face-grooming behavior in the Pitx2/ChR2 mice (Figure 3G, Video clip 1). In contrast, the naturally occuring grooming behavior was lower in Pitx2/Arch mice upon photoinhibition than during OFF epochs (Figure 3O). Together, these results demonstrate the importance of the STN in horizontal and vertical locomotion, and also identify a direct correlation between STN excitation and self-grooming.

Unilateral excitation and inhibition of the STN induce opposite rotations

Next, to further assess the impact of optogenetic manipulations, unilateral STN photostimulation was performed in Pitx2/ChR2 and Pitx2/Arch mice (Figure 4A). First, since unilateral activation or inhibition of the STN is expected to give rise to rotational rather than forward movement, this was scored by comparing ipsilateral and contralateral rotations. Indeed, STN-photostimulation induced a strong rotational behavior. Pitx2/ChR2 mice made a significantly higher number of ipsilateral than contralateral rotations during ON epochs (Figure 4B-C). In contrast, Pitx2/Arch mice made significantly more contralateral than ipsilateral rotations during ON epochs (Figure 4E-F). No rotational behavior was detected for control mice during either ON or OFF epochs (Figure 4D and 4G).

Further, the parameters distance moved and speed were both increased during the rotational movement displayed under control of unilateral STN-photoexcitation in Pitx2/ChR2 mice (Figure 4H-I) while rearing was significantly decreased (Figure 4J). Vertical, but not horizontal movement, thus showed the same result in unilateral and bilateral photoexcitation. Similar to bilateral stimulation, grooming and number of jumps were increased by unilateral stimulation, but only the last was significant (Figure 4K-L). Further, STN inhibition in Pitx2/Arch mice provided by unilateral stimulation replicated the findings from bilateral STN-photoinhibition as the movement parameters distance moved, speed and rearing were all

significantly increased in Pitx2/Arch mice during ON epochs (Figure 4L-N). However, no effect on grooming was observed in Pitx2/Arch mice (Figure 4O).

The results confirmed the importance of the STN for coordinated motor output by demonstrating that manipulation of one of the two STN structures is sufficient to produce measurable affects, similar as is observed clinically in hemiballismus. Indeed, the observation of contralateral rotations during inhibition, and ipsilateral rotations during excitation, is further proof that a hyperactive STN in one hemisphere impairs correct movement on the ipsilateral hemibody. This may occur either by activation of basal ganglia output areas inducing ipsilateral rotations, or by an inhibition of the ipsilateral STN which becomes less active than the contralateral one inducing contralateral rotations.

Optogenetic STN-activation disrupts on-going motor coordination

The potent reduction in movement together with gait abnormalities observed during the open field test of Pitx2/ChR2 mice prompted further analysis of the impact of STN excitation on motor coordination. The ability to sustain on-going motor coordination was assessed in the rotating rotarod and beam tests. Upon training to master maintained walking on the rotating rod throughout a two-minute session, mice were exposed to STN stimulation in four OFF/ON trials (Figure 5A-B). Pitx2/ChR2 and control mice all managed to stay on the rod throughout the entire length of the OFF trials. However, within seconds after STN activation was initiated, all Pitx2/ChR2 mice fell off the rod, giving rise to a strikingly short latency to fall (Figure 5C, Video clip 2). In contrast, all control mice maintained their rod-walking undisturbed (Figure 5D). The disrupting effect on motor coordination was transient and displayed specifically upon photoexcitation, with restored coordination during subsequent OFF trial (Figure 5C).

The potent but transient effect on motor coordination upon STN excitation was subsequently confirmed in the beam walk test (Figure 5E-F). Upon training, three conditions were tested in order to determine how the excitation of the STN would influence the motor coordination necessary to cross the beam: alternated OFF and ON epochs (referred as ALT), continuous stimulation along the beam (referred as CONT) or light stimulation starting few seconds before and during the cross of the beam (referred as PRIOR) (Figure 5E). The results were analyzed and summarized in a neuroscore pre-defined rating scale (Supplementary table 2). The maximum score was 10 points for each condition (5 points for latency to cross + 5 points for hind-foot slips). The lower is the score, the better is the motor performance. During the last condition only (PRIOR), motor coordination was altered to significantly increase the number of paw slips and latency to cross (Figure 5G). No effects upon photo-excitation were

observed in control mice (Figure 5H). These experiments pin-point a direct association between STN excitation and balance, and identifies immediate interruption of on-going motor coordination upon STN excitation.

Discussion

The role of the STN in normal motor regulation has long been assumed as established, however, experimental evidence is sparse. In fact, the natural role of the STN in motor regulation has remained poorly explored. Instead, current knowledge is based primarily on pathological models of PD and verified only indirectly, via either lesioning, genetic inactivation or high-frequency stimulation or DBS, the latter two for which the mechanims remain elusive yet today. But motor function is complex, and improving knowledge of STN´s regulatory role has strong potential to aid towards improved clinical outcome.

By implementing optogenetics, new possibilities to directly compare the behavioral readout upon STN excitation and inhibition has opened up. Based on our previous data showing that 20 Hz photostimulation was sufficient to release glutamate in the GP of Pitx2/ChR2 mice [25], a photoexcitation protocol designed for behavioral motor analysis was formulated. We found that GP neurons were excited already upon a 0.5 Hz STN photostimulation, but our electrophysiological recordings clearly showed that the 20 Hz Behavior protocol gave rise to the majority of excitatory responses. Optogenetic STN excitation and inhibition caused mirrored effects on several aspects of motor function with reduced forward locomotion and rearing upon activation, and enhancement of both parameters upon inhibition. These findings were further potentiated by loss of balance and motor coordination in advanced motor tasks immediately upon STN activation. The strong impact of STN excitation on balance and coordination likely reflects its reducing effect on movement, thus disturbing the ability to maintain position in challenging conditions where flexible motor output is required. Initiation of forward movement as well as balance and coordination are critical motor features needed to enable and sustain voluntary movement, and their dysfunction is a key pathological feature of PD. The experimental approach used in this study enabled the firm identification of a clear correlation between the STN and each of these pivotal motor functions. Further, in the open field test, immediate self-grooming was initiated upon STN excitation. Of particular interest to note is that while the disruption of on-going motor coordination was not a consequence of grooming induced upon STN activation, forward movement and rearing were replaced by self-grooming.

Our study also showed that unilateral STN excitation and inhibition induced ipsilateral and contralateral rotations, respectively. Recently, it was shown that activation of GABA neurons in the GP induced stereotyped movements and contralateral rotation with mice displaying

less moving and exploration, while stimulation of glutamatergic fibers from the STN to the GP induced a similar response but ipsilateral rotations [23]. In the current context, we propose that our observation of grooming might be ascribed to GP modulation upon STN activation, while the rotation bias might be attributed to the recruitment of other targets. We further speculate that our excitation of the STN could induce a direct activation of the EP, resulting in hypolocomotion of the corresponding hemibody and ipsilateral rotations. In contrast, the inhibition of the STN might have led to removal of STN-derived glutamatergic control over the EP with increased movements in the ipsilateral hemibody and contralateral rotations as direct consequence.

Previous reports have shown that inactivation of STN function, either by surgical STN lesioning [29] or by conditional knockout of the gene encoding the Vesicular glutamate transporter 2 (VGLUT2) in the STN of Pitx2-Cre mice [24] significantly elevated the level of locomotion during non-parkinsonian conditions. In addition, the STN-VGLUT2 knockout strategy strongly enhanced rearing behavior [30]. These results thereby supported the current hypothesis that inactivation of the STN should enhance locomotion by weakening the indirect pathway over the direct pathway. Here we showed that optogenetic inhibition of the STN caused hyperkinesia during non-pathological conditions, a finding in accordance with these previous studies [24,30]. Similar to strategies using electrical high-frequency stimulation of the STN, our optogenetics results indirectly support the role of STN inhibition in promoting movement. In contrast, photoexcitation of the STN caused reduced locomotion, a finding further confirmed by loss of motor coordination in advanced motor tasks. These results were distinct from, but in accordance with, a recent study identifying that on-going licking behavior in mice was interrupted by optogenetic excitation of STN neurons [31].

The STN is an essential clinical target in PD intervention via lesioning and, primarily, STN-DBS [32–34]. Despite its current application as treatment of PD with high success rate, the mechanisms behind STN-DBS are still not entirely understood. It is still debated whether the neural elements are excited or inhibited [17,18]. One model of DBS mechanism involves the depolarization of axons and inhibition of cell bodies [35,36] while another proposed mechanism involves the excitation of afferent, efferent and passing fibers [37] with increased firing [38] and glutamate release in basal ganglia output areas [39]. Studies based on optogenetics in parkinsonian animal models have led support to both the inhibition and excitation hypothesis of STN-DBS [10,11,20]. Recently, a study using the ultrafast opsin CHRONOS to create an

animal model of optogenetic STN-DBS model showed that parkinsonian movement disability was improved to a similar degree as when electrical STN-DBS was applied, further strengthening the correlation between the STN and motor output in the parkinsonian context [21].

Beyond PD, the STN is also a new target for DBS treatments in cognitive and affective disorders, including obsessive compulsive disorder (OCD). A surprising result in our study was the display of strongly repetitive face-grooming directly upon STN excitation. While a motoric manifestation, self-grooming can also reflect cognitive and affective functions [40–43]. Indeed, stereotypy, such as repetitive and excessive grooming, is a behavioral criteria for rodent models of OCD, and is commonly interpreted as a rodent equivalent to compulsivity in patients with OCD [44]. Indeed, high-frequency stimulation of the STN has been demonstrated effective in the treatment compulsive-like behaviors in rodents [45,46] and non-human primates [43]. The neurological underpinnings for the STN in compulsive behavior needs further attention. However, it is evident from the current study that STN excitation promotes face grooming. Thus, also in this distinct type of motor output, the STN acts as a gate.

The present study identified directly opposite motor effects as a consequence of STN excitation and inhibition, respectively. Thus, by optogenetically driving STN activity, a direct correlation between this clinically relevant brain nucleus and several motor parameters essential to achieve intended movement, could be pin-pointed. Our study thereby contributes to the current decoding of the role of the STN in normal regulation of movement, and the findings should also prove useful also towards an increased understanding of neurobiological underpinnings of STN-DBS.

Methods

Pitx2-Cre_C57BL/6NTac transgenic mice were bred and housed at the animal facility of Uppsala University throughout the study, except mice transported to University of Bordeaux after virus injections for electrophysiological experiments. All experimental procedures followed Swedish (Animal Welfare Act SFS 1998:56) and European Union Legislation (Convention ETS 123 and Directive 2010/63/EU), and were approved by Uppsala Djurförsöksetiska Nämnd, Sweden, and, for electrophysiology, Le Comité d'Ethique pour l'Expérimentation Animale Bordeaux (N°50120205-A) Ethical Committee, France.

Experimental protocols are outlined in detail in the Online Methods section.

Figure Legends

Figure 1.

Expression of optogenetic constructs in the STN of Pitx2-Cre mice with c-Fos induced upon photoexcitation confirms experimental setup

(A) Timeline of the experimental setup. Left: graphical representation of stereotaxic bilateral injection of rAAV carrying either a Cre-dependent Channelrhodopsin 2 or Archeorhodopsin 3.0 fused with eYFP into the STN of Pitx2-Cre mice; Right: overview of the electrophysiological and behavioral experiments. (B) Simplified representation of the basal ganglia circuitry and associated structures. (C-D) Representative image of eYFP fluorescence (green) in STN cell bodies in Pitx2-Cre mice, including a close-up (D); nuclear marker (DAPI, blue); scale, 500 µm (C) and 250 µm (D). (E-H) Representative images of coronal sections showing eYFP fluorescence (green) in STN neurons target areas projections: (E) VP, (F) GP, (G) GP and EP and (H) SNr and SNc; nuclear marker (DAPI, blue); scale, 250 µm. (I) Example image showing eYFP (green) and c-Fos expression in the STN of Pitx2/ChR2 mice upon 120s photostimulation *in vivo*. (I') High magnification showing colocalization of eYFP and c-Fos positive neurons. (J, J', K, K'). None of the two controls, Pitx2/ChR2 without light stimulation and Pitx2/eYFP-C with light stimulation, showed c-Fos expression in the STN. For (H), (I) and (J), the white rectangles represent the corresponding high magnification pictures.

Abbreviations: STN, subthalamic nucleus; pSTN, para-subthalamic nucleus; VP, ventral pallidum; GP, globus pallidus; EP, entopeduncular nucleus; SNr, substantia nigra *pars reticulata*; SNc, substantia nigra *pars compacta*; Thal, thalamus.

Figure 2. Optogenetic activation excites STN neurons and induces post-synaptic responses within the basal ganglia

(A) Procedure for STN optotagging experiments. (B) Example of a PSTH and raster (trials) of a neuron excited upon light stimulation. (C) Procedure of GP recordings experiments with STN photostimulation. (D) Example of a raster and PSTH of a GP neuron excited by STN photostimulation. (E) Overlapped recorded spikes of a GP neuron triggered by STN photostimulation during the PSTH protocol. (F) z-score of 12 GP neurons excited during the PSTH protocol. (G) Example of an excited GP neuron during a behavioral protocol with the frequency and the recording trace. (H) Firing rate of excited GP neurons before, during and after 100 seconds of light stimulation as shown in g. Results showed a significant difference in the firing rate between "Stimulation" and "Post-stimulation", #$p<0.05$, *$p<0.05$. (I) eYFP

fibers in the GP and sky blue pontamine deposit (red dot) at the last recorded coordinates (scale, 200 µm). (J) Reconstructed mapping of GP recorded neurons at three different antero-posterior levels (N=20 neurons recorded in 3 mice). Dark blue dots indicate neurons excited during the two different protocols (PSTH and Behavior protocols), light blue dots indicate neurons excited during one of the two protocols and white dots correspond to neurons which did not respond to the light. The pie chart shows that about two third of GP neurons were excited upon STN photostimulation. Blue arrow in B, D and E shows STN photostimulation.

Abbreviations: STN, subthalamic nucleus; GP, globus pallidus.

Figure 3. Optogenetic activation and inhibition of the STN induce opposite effects on both horizontal and vertical locomotion.

(A-E) In the open field test, several behaviors representative of vertical and horizontal locomotion were recorded in Pitx2/ChR2 mice and their corresponding Pitx2/eYFP-C control mice: rearing (A), distance moved (B), speed (C), time spent moving (D), times spent exploring the center (E) and center visits (F). (G-H) Graphs showing the time spent grooming (G) and the number of jumps (H). (I-N) The same behavioral parameters were recorded in Pitx2/Arch and Pitx2/eYFP-A control mice: rearing (I), distance moved (J), speed (K), time spent moving (L), time spent exploring the center (M) and visits to the center (N). Time spent grooming (O) was also recorded. All data are presented as average for the two ON and OFF epochs ± SEM, *$p<0.05$, **$p<0.01$, ***$p<0.001$.

Figure 4. Unilateral inhibition and excitation of the STN induce opposite rotations.

(A) Schematic representation of the open field test with unilateral stimulation. (B) Graphic representation of types of body rotations displayed by Pitx2/ChR2 mice depending on stimulated hemisphere. (C-D) Number of ipsilateral and contralateral rotations in Pitx2/ChR2 mice (C) and Pitx2/eYFP-C control mice (D) upon STN photoexcitation. (E) Graphic representation of types of body rotations displayed by Pitx2/Arch mice depending on stimulated hemisphere. (F-G) Number of ipsilateral and contralateral rotations in Pitx2/Arch mice (F) and Pitx2/eYFP-A control mice (G) upon STN photoinhibition. (H-J) Graphs showing horizontal locomotion represented by the distance moved (H) and speed (I) in Pitx2/ChR2 mice and vertical locomotion by rearing (J). (K-L) Graphs showing the time that Pitx2/ChR2 mice spent grooming (K), and the number of jumps (L), upon photoexcitation. (M-N) Graphs showing horizontal locomotion represented by the distance moved (M) and speed (N) and vertical locomotion by rearing (O) in Pitx2/Arch mice. (P) Graph showing the time that

Pitx2/Arch mice spent grooming upon photoinhibition. For all data, ON and OFF epochs from the two phases were pooled together and are presented as mean ±SEM, *p<0.05, **p<0.01, ***p<0.001.

Figure 5. Optogenetic STN-activation disrupts on-going motor coordination

(A) Schematic representation of the fixed speed rotarod assay timeline. (B) Graphical representation of the rotarod assay, with the mouse receiving bilateral optical stimulation during ON trials. (C) Latency to fall from the rotating rod for Pitx2/ChR2 is expressed as mean ±SEM, **p<0.01, ***p<0.001 and (D) for Pitx2/eYFP-C control mice, ±SEM, p=0.1989. (E) Schematic representation of the beam walk test time line. (F) Schematic representation of the tested conditions: "*Baseline*" (BS), "*Alternated Light*" (ALT), "*Continuous Light*" (CONT) and "*Prior Stimulation*" (PRIOR). (G-H) The neuroscore is calculated from a scoring scale (see Supplementary Table 2) and is expressed as mean ±SEM, *p<0.05, **p<0.01.

Video clip 1

Video clip of the open filed test showing first a Pitx2/ChR2 mouse in the arena without light stimulation, and second, the same mouse grooming seconds after STN photoexcitation initiated. A close-up video shows the grooming behavior from the side.

Video clip 2

Video clip of the rotarod test showing first a Pitx2/ChR2 mouse walking on the rod without STN photoexcitation (OFF trial) and second, the same mouse falling off the rod few seconds after STN photoexcitation initiated (ON trial, repeated one time at the end of the video clip).

<u>Supplementary tables</u>

Supplementary Table 1

Detailed description of the statistics used for the different experiments with reference to each figure where the data is displayed.

Abbreviations: STN, subthalamic nucleus; GP, globus pallidus; OFT, open field test; BWT, beam walk test.

Supplementary Table 2

Table shows the parameters used to calculate the neuroscore for the beam walking test. Based on Korenova et al., 2009 and adapted for mice [47].

Acknowledgements: We thank Professor James Martin, Baylor College of Medicine, Houston, Texas, USA, for generously providing the Pitx2-Cre transgenic mouse line. Bianca Vlcek and Niclas König of the MackenzieLab are thanked for constructive feedback on the manuscript.

Authors' Roles: A.G: Designed and performed experiments, analyzed data, prepared figures, wrote manuscript; G-P.S: Designed and performed experiments, analyzed data, prepared figures, wrote manuscript; F.G: Supervised electrophysiolgical experiments, analyzed data; Å.W.M: Designed and supervised study; prepared figures; wrote manuscript.

Financial disclosure statement (for the preceding 12 months): A.G (PhD student), G-P.S (Researcher) and Å.M (Professor/Chair) are all employed by Uppsala University. Faculty funding and external grants to Å.M support all activities. External grants: the Swedish Research Council (SMRC 2017-02039), the Swedish Brain Foundation (Hjärnfonden), Parkinsonfonden, and the Research Foundations of Bertil Hållsten, Zoologiska and Åhlén. FG (Research director) is employed by CNRS. CNRS funding support FG salary.

References

1. Nambu A, Tokuno H, Takada M. Functional significance of the corticoÁ/subthalamoÁ/pallidal ‘hyperdirect’ pathway. *Neurosci Res*. Published online 2002:7.

2. Sano H, Chiken S, Hikida T, Kobayashi K, Nambu A. Signals through the Striatopallidal Indirect Pathway Stop Movements by Phasic Excitation in the Substantia Nigra. *J Neurosci*. 2013;33(17):7583-7594. doi:10.1523/JNEUROSCI.4932-12.2013

3. Schmidt R, Berke JD. A Pause-then-Cancel model of stopping: evidence from basal ganglia neurophysiology. *Philos Trans R Soc B Biol Sci*. 2017;372(1718):20160202. doi:10.1098/rstb.2016.0202

4. Kita H, Kitai ST. Efferent projections of the subthalamic nucleus in the rat: Light and electron microscopic analysis with the PHA-L method. *J Comp Neurol*. 1987;260(3):435-452. doi:10.1002/cne.902600309

5. Groenewegen HJ, Berendse HW. Connections of the subthalamic nucleus with ventral striatopallidal parts of the basal ganglia in the rat. *J Comp Neurol*. 1990;294(4):607-622. doi:10.1002/cne.902940408

6. Parent A, Hazrati L-N. Functional anatomy of the basal ganglia. II. The place of subthalamic nucleus and external pallidum in basal ganglia circuitry. :27.

7. Féger J, Bevan M, Crossman AR. The projections from the parafascicular thalamic nucleus to the subthalamic nucleus and the striatum arise from separate neuronal

populations: A comparison with the corticostriatal and corticosubthalamic efferents in a retrograde fluorescent double-labelling study. *Neuroscience*. 1994;60(1):125-132. doi:10.1016/0306-4522(94)90208-9

8. Mouroux M, Féger J. Evidence that the parafascicular nucleus projection to the subthalamic nucleus is glutamatergic. *NeuroReport*. 1993;4(6):613-615. doi:10.1097/00001756-199306000-00002

9. Sugimoto T, Hattori T. Confirmation of thalamosubthalamic projections by electron microscopic autoradiography. *Brain Res*. 1983;267(2):335-339. doi:10.1016/0006-8993(83)90885-5

10. Sanders TH, Jaeger D. Optogenetic stimulation of cortico-subthalamic projections is sufficient to ameliorate bradykinesia in 6-ohda lesioned mice. *Neurobiol Dis*. 2016;95:225-237. doi:10.1016/j.nbd.2016.07.021

11. Gradinaru V, Mogri M, Thompson KR, Henderson JM, Deisseroth K. Optical Deconstruction of Parkinsonian Neural Circuitry. 2009;324:7.

12. Hamada I, DeLong MR. Excitotoxic acid lesions of the primate subthalamic nucleus result in transient dyskinesias of the contralateral limbs. *J Neurophysiol*. 1992;68(5):1850-1858. doi:10.1152/jn.1992.68.5.1850

13. Heywood P, Gill S. Bilateral dorsolateral subthalamotomy for advanced Parkinson's disease. *The Lancet*. 1997;350(9086):1224. doi:10.1016/S0140-6736(05)63455-1

14. Parkin S, Nandi D, Giladi N, et al. Lesioning the Subthalamic Nucleus in the Treatment of Parkinson's Disease. *Stereotact Funct Neurosurg*. 2001;77(1-4):68-72. doi:10.1159/000064599

15. Benabid AL. Deep brain stimulation for Parkinson's disease. *Curr Opin Neurobiol*. 2003;13(6):696-706. doi:10.1016/j.conb.2003.11.001

16. Meissner W, Leblois A, Hansel D, et al. Subthalamic high frequency stimulation resets subthalamic firing and reduces abnormal oscillations. *Brain*. 2005;128(10):2372-2382. doi:10.1093/brain/awh616

17. Deniau J-M, Degos B, Bosch C, Maurice N. Deep brain stimulation mechanisms: beyond the concept of local functional inhibition: Deep brain stimulation mechanisms. *Eur J Neurosci*. 2010;32(7):1080-1091. doi:10.1111/j.1460-9568.2010.07413.x

18. Chiken S, Nambu A. Mechanism of Deep Brain Stimulation: Inhibition, Excitation, or Disruption? *The Neuroscientist*. 2016;22(3):313-322. doi:10.1177/1073858415581986

19. Deisseroth K. Optogenetics. *Nat Methods*. 2011;8(1):26-29. doi:10.1038/nmeth.f.324

20. Yoon HH, Park JH, Kim YH, et al. Optogenetic Inactivation of the Subthalamic Nucleus Improves Forelimb Akinesia in a Rat Model of Parkinson Disease: *Neurosurgery*. 2014;74(5):533-541. doi:10.1227/NEU.0000000000000297

21. Yu C, Cassar IR, Sambangi J, Grill WM. Frequency-Specific Optogenetic Deep Brain Stimulation of Subthalamic Nucleus Improves Parkinsonian Motor Behaviors. *J Neurosci*. Published online April 20, 2020:JN-RM-3071-19. doi:10.1523/JNEUROSCI.3071-19.2020

22. Kravitz AV, Freeze BS, Parker PRL, et al. Regulation of parkinsonian motor behaviours by optogenetic control of basal ganglia circuitry. *Nature*. 2010;466(7306):622-626. doi:10.1038/nature09159

23. Tian J, Yan Y, Xi W, et al. Optogenetic Stimulation of GABAergic Neurons in the Globus Pallidus Produces Hyperkinesia. *Front Behav Neurosci*. 2018;12:185. doi:10.3389/fnbeh.2018.00185

24. Schweizer N, Pupe S, Arvidsson E, et al. Limiting glutamate transmission in a Vglut2-expressing subpopulation of the subthalamic nucleus is sufficient to cause hyperlocomotion. *Proc Natl Acad Sci*. 2014;111(21):7837-7842. doi:10.1073/pnas.1323499111

25. Viereckel T, Konradsson-Geuken Å, Wallén-Mackenzie Å. Validated multi-step approach for *in vivo* recording and analysis of optogenetically evoked glutamate in the mouse globus pallidus. *J Neurochem*. 2018;145(2):125-138. doi:10.1111/jnc.14288

26. Martin DM, Skidmore JM, Philips ST, et al. PITX2 is required for normal development of neurons in the mouse subthalamic nucleus and midbrain. *Dev Biol*. 2004;267(1):93-108. doi:10.1016/j.ydbio.2003.10.035

27. Skidmore JM, Cramer JD, Martin JF, Martin DM. Cre fate mapping reveals lineage specific defects in neuronal migration with loss of Pitx2 function in the developing mouse hypothalamus and subthalamic nucleus. *Mol Cell Neurosci*. 2008;37(4):696-707. doi:10.1016/j.mcn.2007.12.015

28. Schweizer, Viereckel, Smith-Anttila, et al. Reduced *Vglut2/Slc17a6* Gene Expression Levels throughout the Mouse Subthalamic Nucleus Cause Cell Loss and Structural Disorganization Followed by Increased Motor Activity and Decreased Sugar Consumption. *eneuro*. 2016;3(5):ENEURO.0264-16.2016. doi:10.1523/ENEURO.0264-16.2016

29. Alvarez L. Bilateral subthalamotomy in Parkinson's disease: initial and long-term response. *Brain*. 2005;128(3):570-583. doi:10.1093/brain/awh397

30. Schweizer N, Viereckel T, Smith-Anttila CJA, et al. Reduced Vglut2/Slc17a6 Gene Expression Levels throughout the Mouse Subthalamic Nucleus Cause Cell Loss and Structural Disorganization Followed by Increased Motor Activity and Decreased Sugar Consumption. *eNeuro*. 2016;3(5). doi:10.1523/ENEURO.0264-16.2016

31. Fife KH, Gutierrez-Reed NA, Zell V, et al. Causal role for the subthalamic nucleus in interrupting behavior. *eLife*. 2017;6. doi:10.7554/eLife.27689

32. Bergman H, Wichmann T, DeLong M. Reversal of experimental parkinsonism by lesions of the subthalamic nucleus. *Science*. 1990;249(4975):1436-1438. doi:10.1126/science.2402638

33. Benabid AL, Pollak P, Hoffmann D, et al. Long-term suppression of tremor by chronic stimulation of the ventral intermediate thalamic nucleus. *The Lancet*. 1991;337(8738):403-406. doi:10.1016/0140-6736(91)91175-T

34. Limousin P, Pollak P, Benazzouz A, et al. Effect on parkinsonian signs and symptoms of bilateral subthalamic nucleus stimulation. *The Lancet*. 1995;345(8942):91-95. doi:10.1016/S0140-6736(95)90062-4

35. Vitek JL. Mechanisms of deep brain stimulation: Excitation or inhibition. *Mov Disord*. 2002;17(S3):S69-S72. doi:10.1002/mds.10144

36. Florence G, Sameshima K, Fonoff ET, Hamani C. Deep Brain Stimulation: More Complex than the Inhibition of Cells and Excitation of Fibers. *The Neuroscientist*. 2016;22(4):332-345. doi:10.1177/1073858415591964

37. Kringelbach ML, Jenkinson N, Owen SLF, Aziz TZ. Translational principles of deep brain stimulation. *Nat Rev Neurosci*. 2007;8(8):623-635. doi:10.1038/nrn2196

38. Hashimoto T, Elder CM, Okun MS, Patrick SK, Vitek JL. Stimulation of the Subthalamic Nucleus Changes the Firing Pattern of Pallidal Neurons. *J Neurosci*. 2003;23(5):1916-1923. doi:10.1523/JNEUROSCI.23-05-01916.2003

39. Windels F, Bruet N, Poupard A, et al. Effects of high frequency stimulation of subthalamic nucleus on extracellular glutamate and GABA in substantia nigra and globus pallidus in the normal rat: STN HFS and neurochemical changes in GP and SNr. *Eur J Neurosci*. 2000;12(11):4141-4146. doi:10.1046/j.1460-9568.2000.00296.x

40. Baunez C, Robbins TW. Bilateral Lesions of the Subthalamic Nucleus Induce Multiple Deficits in an Attentional Task in Rats. *Eur J Neurosci*. 1997;9(10):2086-2099. doi:10.1111/j.1460-9568.1997.tb01376.x

41. Mallet L, Mesnage V, Houeto J-L, et al. Compulsions, Parkinson's disease, and stimulation. *The Lancet*. 2002;360(9342):1302-1304. doi:10.1016/S0140-6736(02)11339-0

42. Mallet L, Polosan M, Jaafari N, et al. Subthalamic Nucleus Stimulation in Severe Obsessive–Compulsive Disorder. *N Engl J Med*. 2008;359(20):2121-2134. doi:10.1056/NEJMoa0708514

43. Baup N, Grabli D, Karachi C, et al. High-Frequency Stimulation of the Anterior Subthalamic Nucleus Reduces Stereotyped Behaviors in Primates. *J Neurosci*. 2008;28(35):8785-8788. doi:10.1523/JNEUROSCI.2384-08.2008

44. Kalueff AV, Stewart AM, Song C, Berridge KC, Graybiel AM, Fentress JC. Neurobiology of rodent self-grooming and its value for translational neuroscience. *Nat Rev Neurosci*. 2016;17(1):45-59. doi:10.1038/nrn.2015.8

45. Winter C, Flash S, Klavir O, Klein J, Sohr R, Joel D. The role of the subthalamic nucleus in 'compulsive' behavior in rats. *Eur J Neurosci*. 2008;27(8):1902-1911. doi:10.1111/j.1460-9568.2008.06148.x

46. Klavir O, Flash S, Winter C, Joel D. High frequency stimulation and pharmacological inactivation of the subthalamic nucleus reduces 'compulsive' lever-pressing in rats. *Exp Neurol*. 2009;215(1):101-109. doi:10.1016/j.expneurol.2008.09.017

47. Korenova M, Zilka N, Stozicka Z, Bugos O, Vanicky I, Novak M. NeuroScale, the battery of behavioral tests with novel scoring system for phenotyping of transgenic rat model of tauopathy. *J Neurosci Methods*. 2009;177(1):108-114. doi:10.1016/j.jneumeth.2008.09.027

Experimental timeline

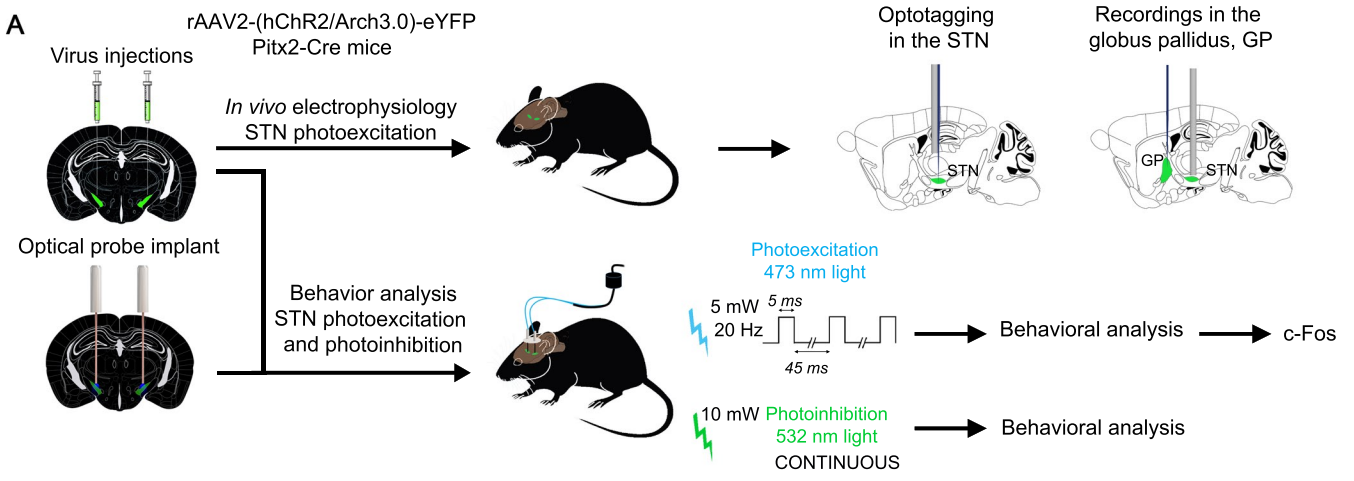

Histological eYFP validation

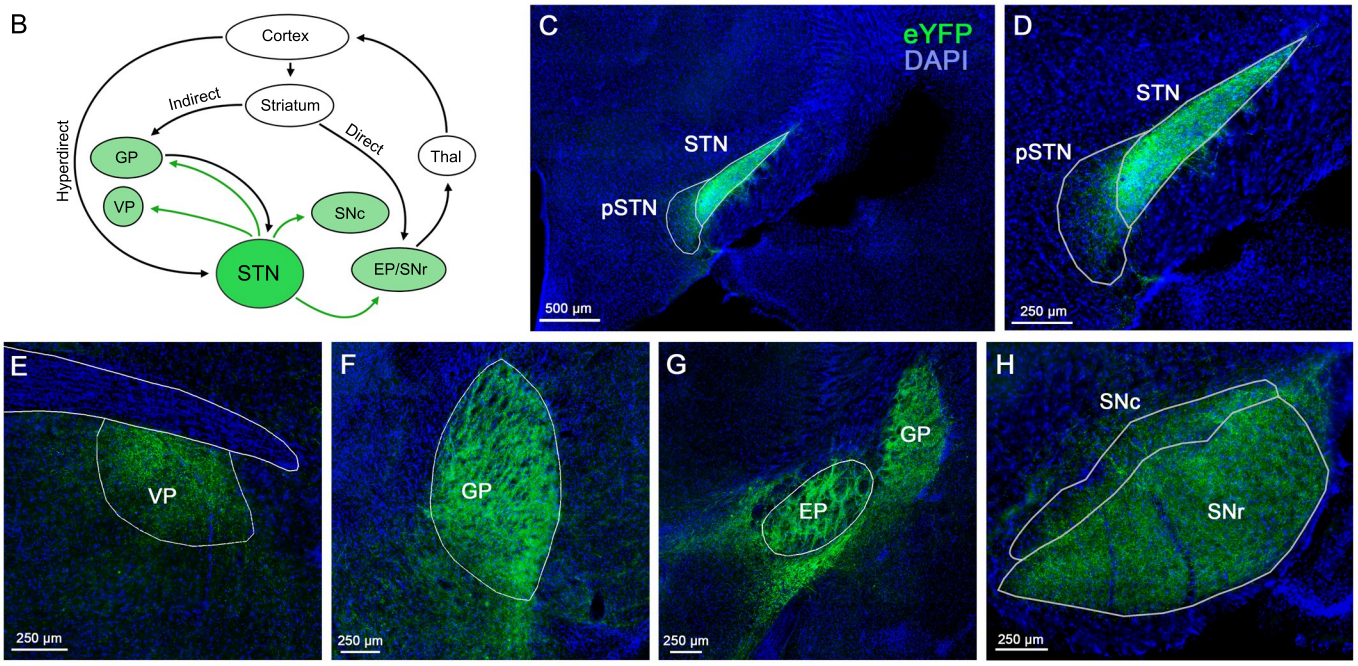

c-Fos

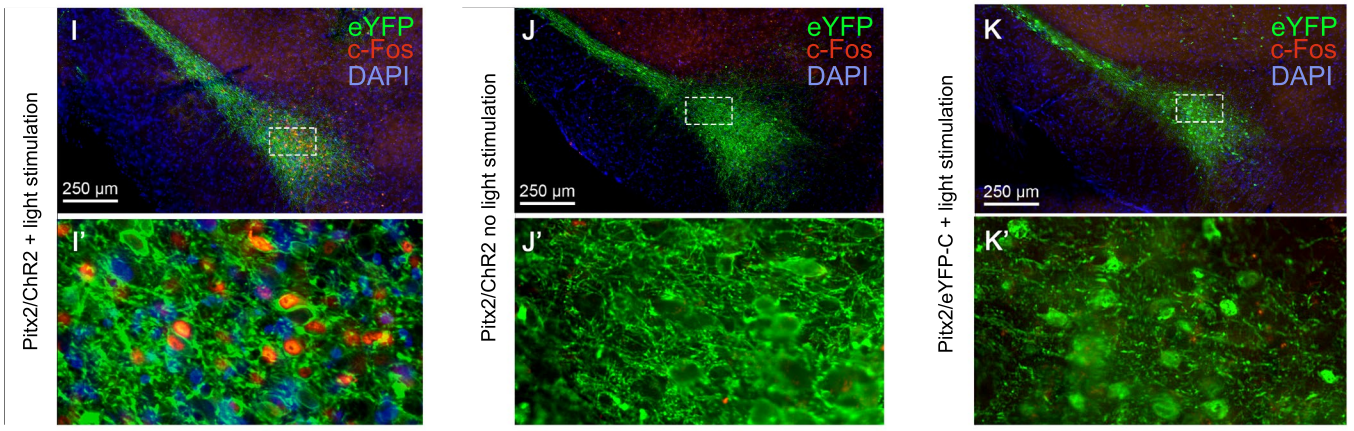

Optotagging in the STN

A

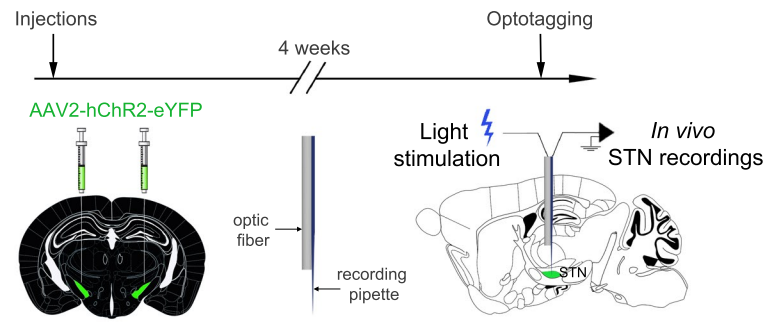

B

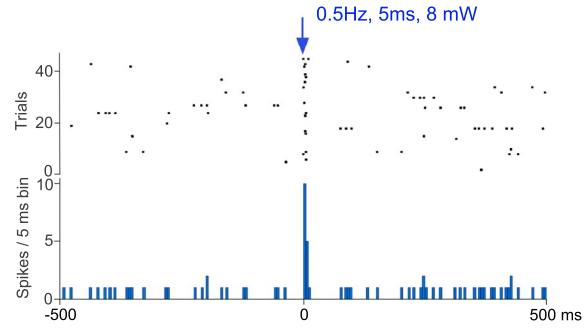

In vivo recordings in the globus pallidus, GP

C

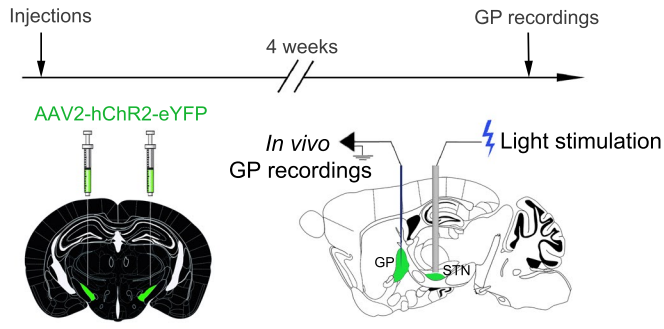

D

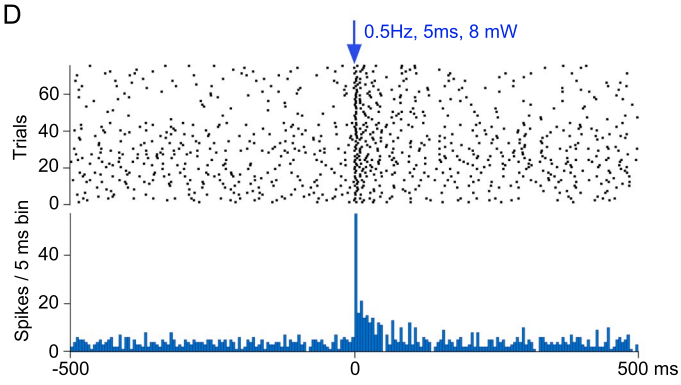

E

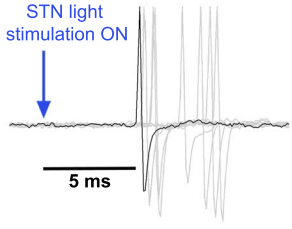

F

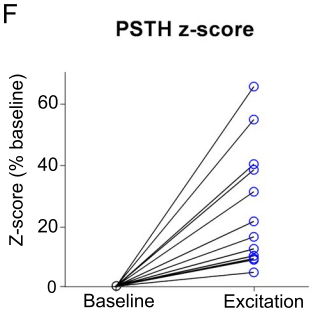

G

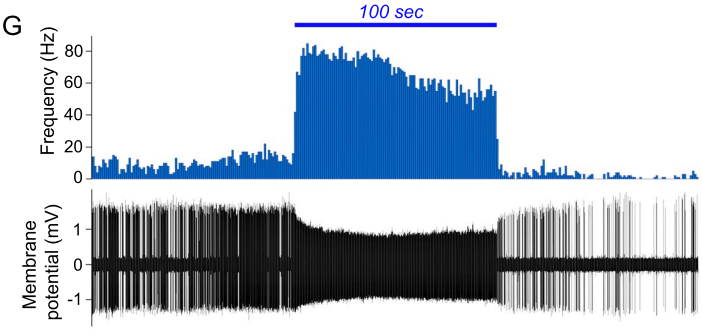

H

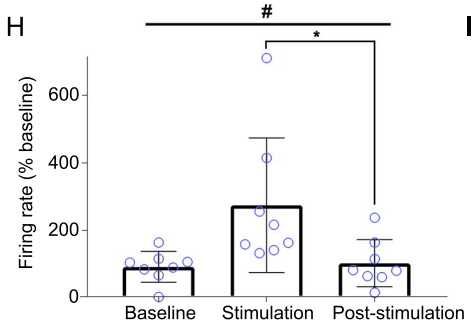

I

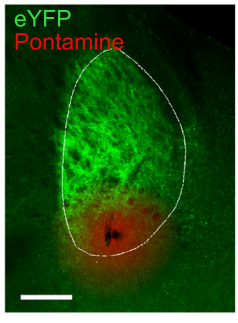

J

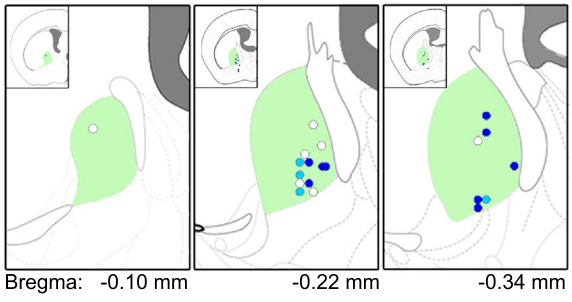

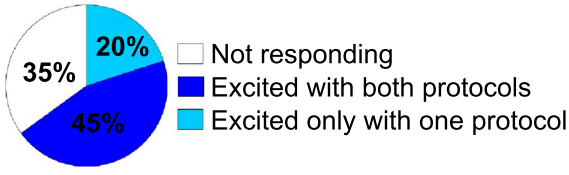

Open Field Test

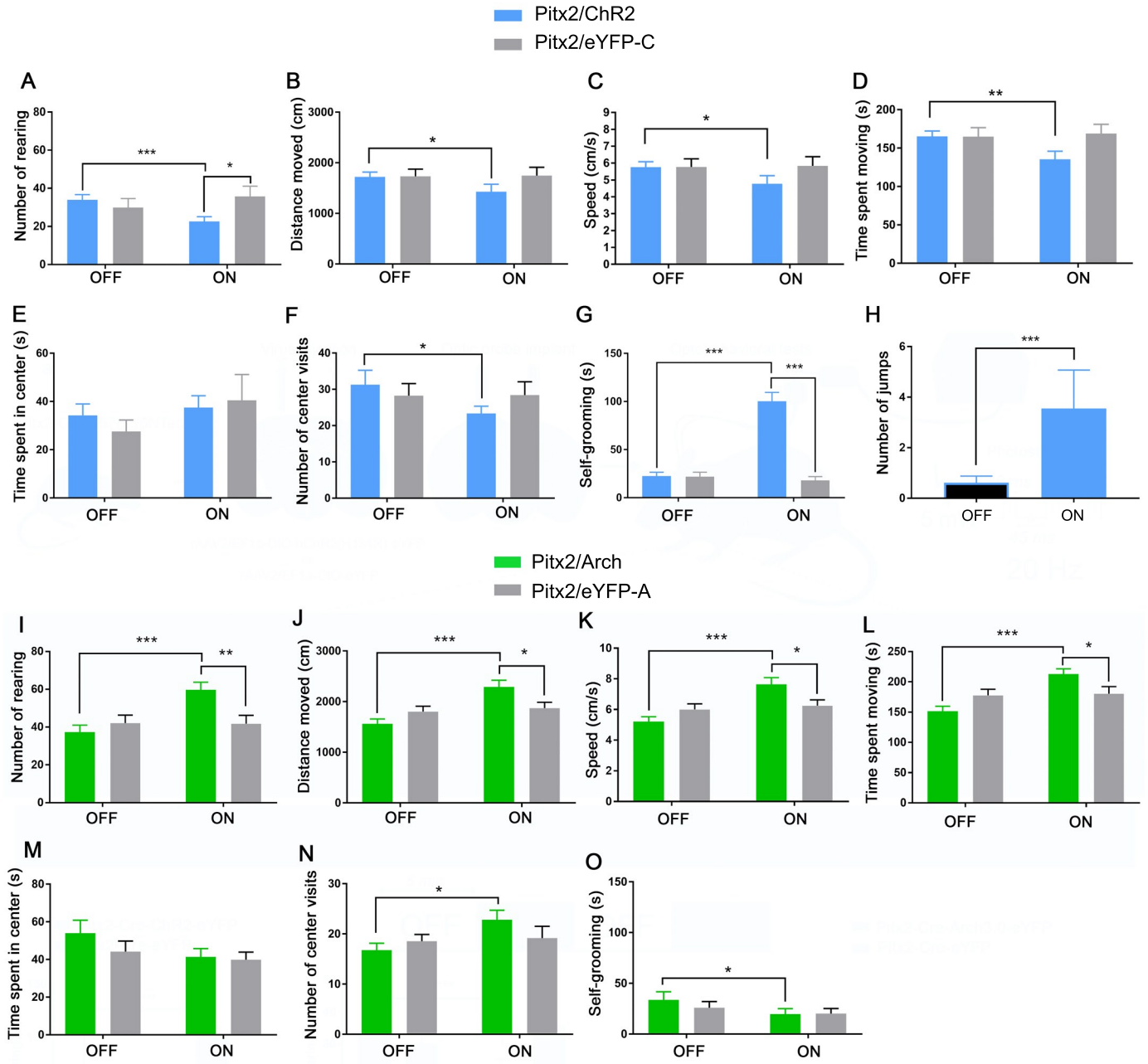

Open Field Test - Unilateral Stimulation

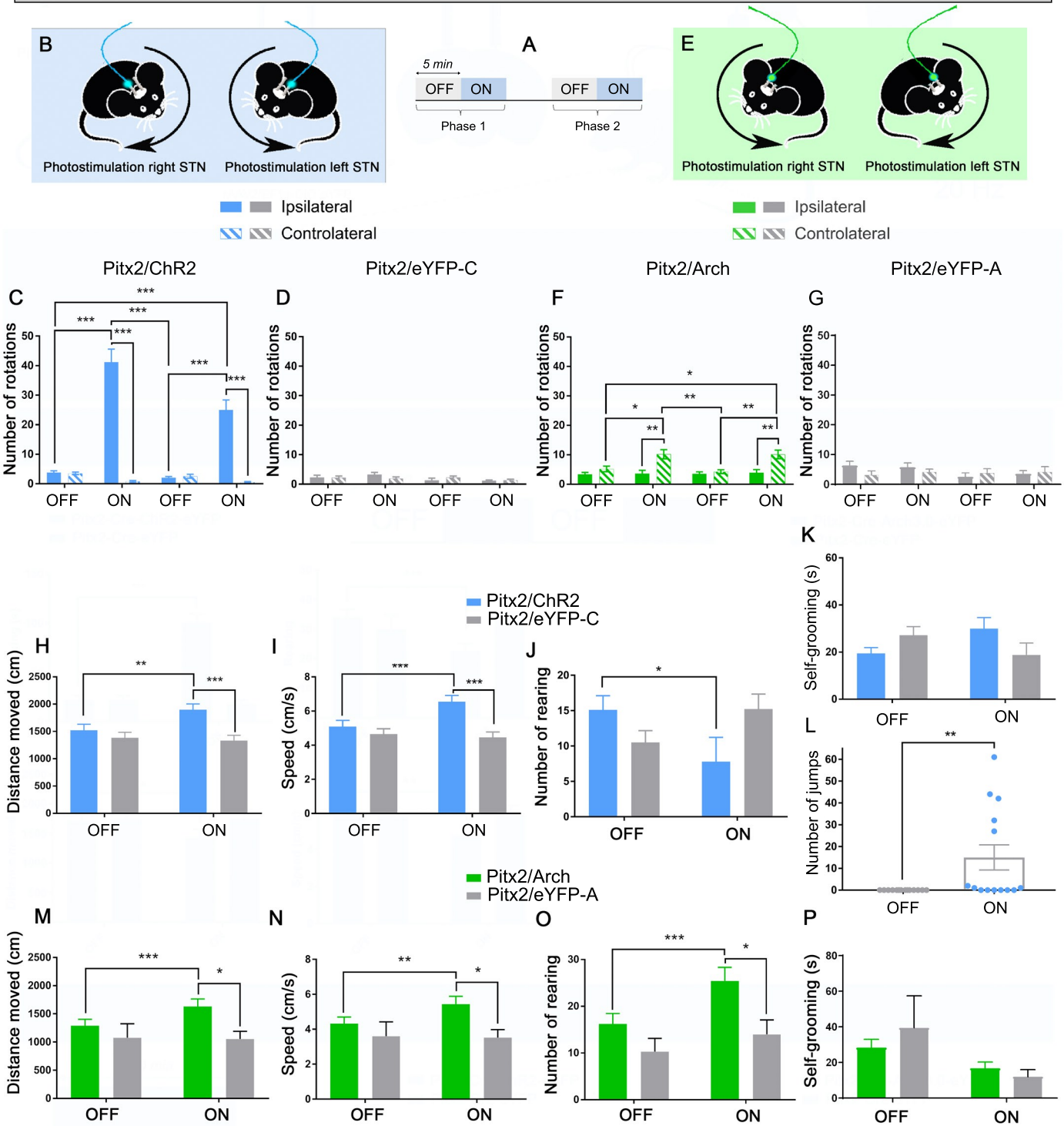

Rotarod

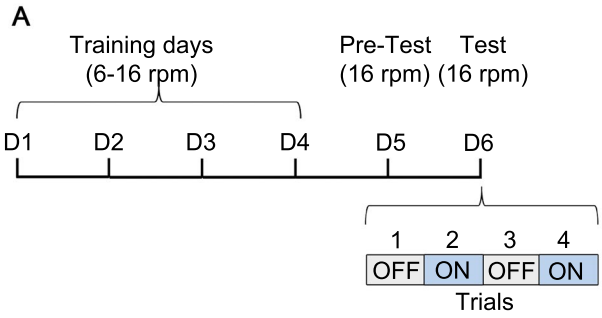

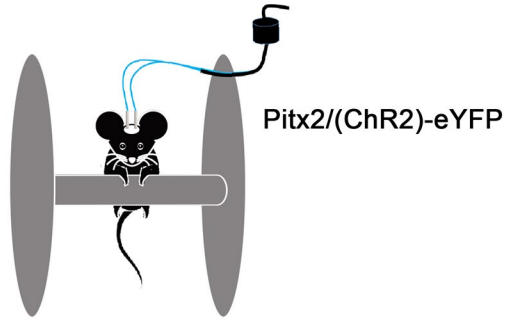

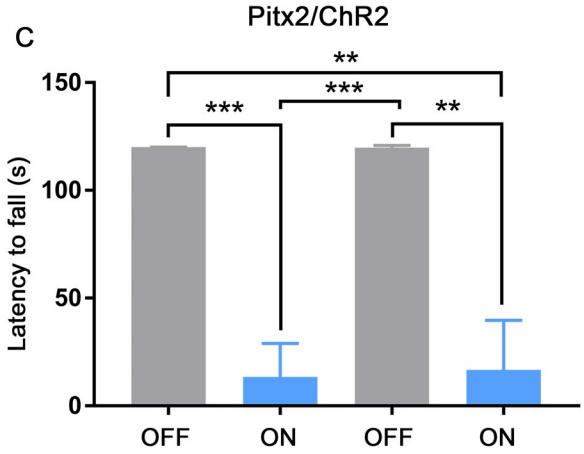

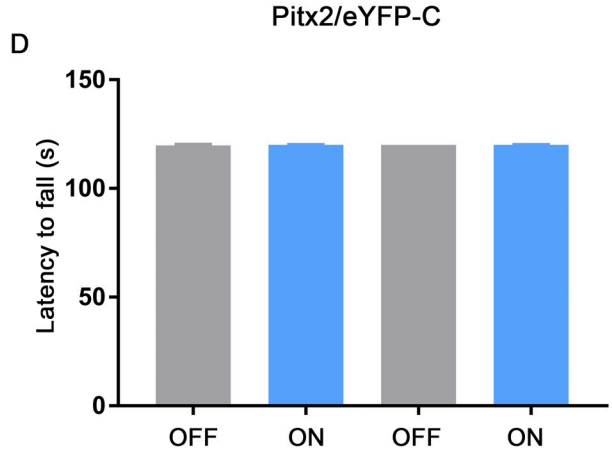

Beam Walk Test

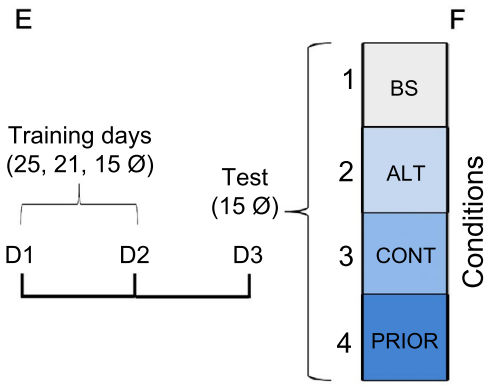

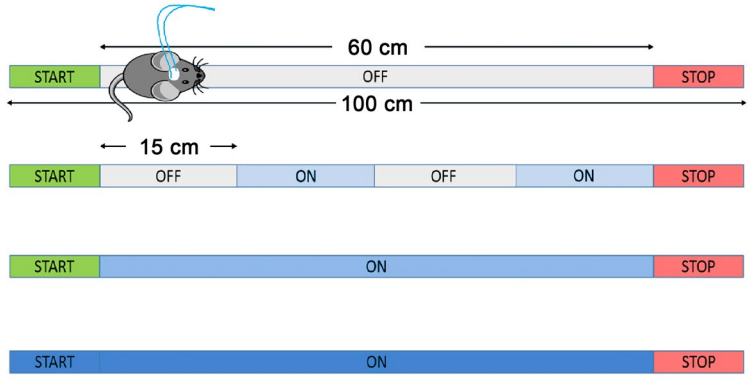

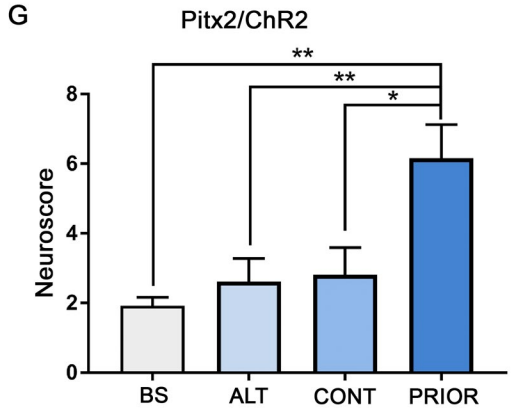

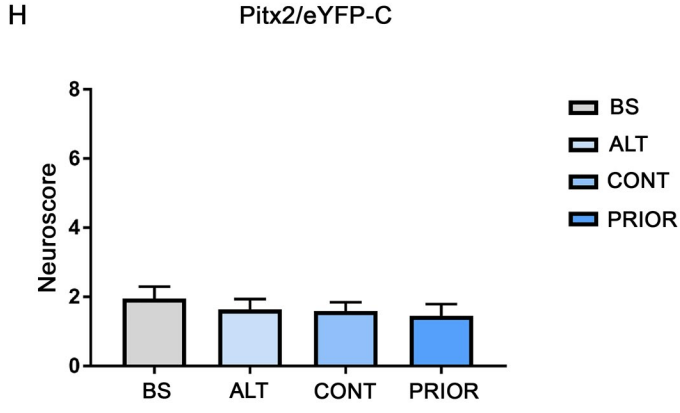

ONLINE METHODS SECTION

Animal housing and ethical permits

Pitx2-Cre_C57BL/6NTac transgenic mice were bred in-house and housed at the animal facility of Uppsala University before and during behavioral experiments or at University of Bordeaux after virus injections for *in vivo* electrophysiological experiments. Mice had access to food and water *ad libitum* in standard humidity and temperature conditions and with a 12 hour dark/light cycle. PCR analyses were run to confirm the genotype of Pitx2-Cre positive mice from ear biopsies. All animal experimental procedures followed Swedish (Animal Welfare Act SFS 1998:56) and European Union Legislation (Convention ETS 123 and Directive 2010/63/EU) and were approved by local Uppsala or Bordeaux (N°50120205-A) Ethical Committee.

Stereotaxic Virus Injection and Optic Cannula Implantation

Virus injection: Stereotaxic injections were performed on anesthetized Pitx2-Cre mice maintained at 1.4-1.8 % (0.5-2 L/min, isoflurane-air mix v/v). Before starting the surgery and 24h post-surgery mice received subcutaneous injection of Carprofen (5 mg/Kg, Norocarp). A topical analgesic, Marcain (1.5 mg/kg; AstraZeneca) was locally injected on the site of the incision. After exposing the skull, holes were drilled in the skull for virus injections and skull screws implantations for behavioral experiments. Mice were injected in the STN bilaterally with a virus containing either a Cre-dependent channelrhodopsin (rAAV2/EF1a-DIO-hChR2(H134R)-eYFP) (mice referred to as Pitx2/ChR2 mice), a Cre-dependent archaerhodopsin (rAAV2/EF1a-DIO-eArch3.0-eYFP) (mice referred to as Pitx2/Arch) or an empty virus carrying only a fluorescent protein (rAAV2/EF1a-DIO-eYFP) (mice referred to as Pitx2/eYFP-C for controls whithin the ChR2 group, and Pitx2/eYFP-A for controls within the Arch group): x $3.8x10^{12}$ virus molecules/mL, $2.7x10^{12}$ virus molecules/mL, $4.6x10^{12}$ virus molecules/mL, respectively (UNC Vector Core, Chapel Hill, NC, USA). The following coordinates were used (adapted from Paxinos and Franklin, 2013): anteroposterior (AP) = -1.90 mm, mediolateral (ML) = +/- 1.70 mm from the midline. 250 nL of virus was injected with a NanoFil syringe (World Precision Instruments, Sarasota, FL, USA) at two dorsoventral levels (DV) = -4.65 mm and -4.25 mm from the dura matter at 100 nL.min-1.

Optic cannula implantation: Optic cannulas (MFC_200/245-0.37_5mm_ZF1.25_FLT, Doric Lenses) were implanted directly after the virus injections. Two skull screws were implanted in the skull to hold the optic cannula-cement-skull complex. Primers (Optibond™ FL, Kerr) were then applied and harden with UV light . Optic cannulas were implanted bilaterally above the STN and fixed with dental cement, coordinates: AP = -1.90 mm, ML = +/- 1.70 mm from the

midline DV = -4.30 mm. 1 mL of saline was injected subcutaneously at the end of the surgery.

Single-Cell Extracellular Recordings

Surgery: *In vivo* single cell extracellular recordings started at least 4 weeks after virus injections. Mice were anesthetized with a mix isoflurane-air (0.8-1.8 % v/v) and placed in a stereotaxic apparatus. Optic fibre, optrode and glass micropipettes coordinates were AP = -1.90 mm, ML = +/- 1.70 mm and DV = -4.30 mm for the STN and respectively anterior and central GP: AP = -0.11 mm relative to bregma, ML = +/- 1.50 mm from sagittal vein, DV = from -3.00 to -5.50 mm depth and AP = -0.71 mm relative to bregma, ML = +/- 1.80 mm, DV: -3.00/-4.20 mm.

STN Optotagging: a custom-made optrode was made with an optic fibre (100 µm diameter, Thorlabs) connected to a laser (MBL-III-473 nm-100 mW laser, CNI Lasers, Changchun, China) mounted and glued on the recording glass micropipette which was filled with 2% pontamine sky blue in 0.5 µM sodium acetate (tip diameter 1-2 µm, resistance 10-15 MΩ). The distance between the end of the optic fibre and the tip of the recording pipette varied between 650 nm and 950 nm. Extracellular action potentials were recorded and amplified with an Axoclamp-2B and filtered (300 Hz/0.5 kHz). Single extracellular spikes were collected online (CED 1401, SPIKE2; Cambridge Electronic Design). The laser power was measured before starting each experiment using a power meter (Thorlabs). The baseline was recorded for 100 seconds for each neuron before starting any light stimulation protocols which were set and triggered with Spike2 software. Light protocol consisted in a peristimulus time histogram (PSTH, 0.5 Hz, 5 ms bin width, 5-8 mW) for at least 100 seconds.

GP recordings: an optic fibre was placed above the STN and GP neurons were recorded. For each GP neurons, a PSTH was recorded upon STN optogenetic stimulation (PSTH 0.5 Hz, 5 ms pulses, 5-8 mW) for at least 100 seconds. Once the neuronal activity returned to baseline the same light stimulation protocol used in behavioral experiments was applied for 100 seconds (20 Hz, 5 ms pulses, 5-8 mW, referred as “behavioral protocol”). Neurons are considered as excited during the PSTH protocol when, following the light pulses centered on 0, the number of spikes/5ms bin is higher than the baseline (-500 ms to 0 ms) plus two times the standard deviation.

Histology: At the end of each experiment a deposit was made at the last recording coordinates by pontamine sky blue electrophoresis (−20 µA, 25 min). Brains were then collected after 0.9% NaCl and 4% PFA transcardial perfusion. 60 µm brain sections were cut with a vibratome at the levels of the STN and the GP, mounted with Vectashield medium

(Vector Laboratories), coverslipped and visualized with an epifluorescent microscope to confirm eYFP expression, recording pipette and optic fibre positions.

c-Fos Activation

Pitx2/ChR2 and respective Pitx2/eYFP-C control mice were connected to the optic fibre and put in a neutral cage for 20 min before receiving 2 min light stimulation, 5 mW, 5 ms pulse duration, 20 Hz. Mice were perfused 90 min after the light stimulation.

Histological Analysis

Following behavioral tests, mice were deeply anesthetized and perfused transcardially with Phosphate-Buffer-Saline (PBS) followed by ice-cold 4% formaldehyde. Brains were extracted and 60 µm sections were cut with a vibratome. Immunohistochemistry for eYFP expression was run on sections from every mice and immunohistochemistry for c-Fos expression was run on sections of mice which underwent a c-Fos activation protocol. After mounting, slices were scanned with NanoZoomer 2-0-HT.0 (Hamamatsu) scanner and visualized with NDPView2 software (Hamamatsu).

Fluorescent immunohistochemistry was performed to reveal c-Fos expression and enhance eYFP signal. After rinsing in PBS, sections were incubated for 90 min in PBS 0.3% X-100 Triton containing 10% blocking solution (normal donkey serum) followed by an incubation with primary antibodies, diluted in 1% normal donkey serum in PBS, overnight at 4°C (chicken anti-GFP 1:1000, cat. no. ab13970, Abcam; rabbit anti-c-Fos 1:800, cat. no. 226003, Synaptic System). The next day sections were rinsed in PBS plus 0.1% Tween-20 solution and incubated for 90 min with secondary antibodies diluted in PBS (Cy3 donkey anti-rabbit 1:1000; A488 donkey anti-chicken 1:1000, cat. no. 703-545-155, Jackson Immunoresearch). After rinsing in PBS plus 0.1% Tween-20 solution, sections were incubated for 30 min with DAPI diluted in distilled water (1:5000). Sections were mounted with Fluoromount Aqueous mounting medium (Sigma, USA) and cover-slipped.

Behavioral Testing

After approximately 4 weeks of recovering from surgery, mice were analyzed in validated behavioral paradigms, during which the same stimulation protocols were used: for Pitx2/ChR2 and respective controls, 473 nm light, 5 mW, 20 Hz, 5 ms pulse delivered by a MBL-III-473 nm-100 mW laser (CNI Lasers, Changchun, China); for Pitx2/Arch and respective controls, 532 nm continuous light, 10 mW, delivered by a MBL-III-532 nm-100 mW laser (CNI Lasers, Changchun, China). Duration and condition of stimulation were specified for each test. After completed behavioral tests, mice were sacrificed and brains analyzed histologically and for placement of optic cannulas. Mice in which the optic cannulas were not in correct position were excluded from the analysis.

Habituation

3 weeks after surgery and before the first behavioral test, all mice were handled and habituated to the experimental room and to the optic cables to reduce the stress during the day of the experiment. Before each behavioral test, mice were acclimatized for 30 minutes in the experimental room.

Open Field Test

Mice were individually placed in neutral cages for 3 minutes in order to recover after connecting the optic cables. Mice were subsequently placed in the central zone of the open field arena and allowed to freely explore it for 5 min before starting the test. The open-field chamber consisted in a 50 cm, squared, transparent, plastic arena with a white floor that has been divided into a central zone (center, 25% of the total area) and a peripheral zone (borders). The Open Field Test consisted of a 20 minutes session divided in four alternating 5-minutes trials (OFF-ON-OFF-ON). The patch cable was connected to a rotary joint, which was attached on the other end to a laser that was controlled by an Arduino Uno card. During the light ON trials, blue light was delivered according to the behavioral stimulation protocol. Total distance moved, speed, time spent and frequency in crossing to the center and body elongation, were automatically documented. Rearing, grooming and escape behavior were manually recorded by an experimenter blind to the experimental groups using the EthoVision XT 12.0/13.0 tracking software (Noldus Information Technology, The Netherlands).

Unilateral STN-Stimulation in the Open Field

The test was performed in the same testing arena used for the Open Field Test and consisted of two 10-minute phases, each divided in two 5-minute trials (OFF-ON). Light was delivered during ON trials according to the protocol. On "*Phase 1*" the photostimulation was randomly paired to one hemisphere while on "*Phase 2*" it was delivered to the contralateral hemisphere. Before "*Phase 1*", mice were allowed to recover from handling in a neutral cage for 5 minutes, then they were placed in the center of the arena and allowed to explore it for 5 minutes before starting the test. Between the two phases the optic fiber was switched from one hemisphere to the contralateral one. Again mice were allowed to recover from handling in a neutral cage for 5 minutes and then placed in the center of the arena for "*Phase 2*". Total distance moved, body rotations, time spent and frequency in crossing to the center of the arena were automatically recorded while rearing activity, grooming and escape behavior were manually scored by using the EthoVision XT 13.0 tracking software (Noldus Information Technology, The Netherlands).

Rotarod

A fixed-speed rotarod assay was performed to investigate the ability of mice to maintain balance on a rotating rod (BIOSEB, Vitrolles, France). Before testing, all animals were trained for 4 days ("*Training Days")* on different trials with fixed-speed protocols (6, 8, 12, 16 rpm). Each trial consisted of a maximum of 3 attempts. Mice were individually placed in a neutral cage to recover from connection for 15 min before starting the trial. Each trial was considered to have started after 5 s that the mouse was placed on the rotating drum and ended either when the mouse fell from the rod or after a total time of 120 s had elapsed. Resting time between trials was 5 min. Once an animal succeeded to stay on the rod for 120 s it was approved to the next trial according to the daily schedule. The "*Pre Test*" day consisted of 4 trials at a fixed speed of 16 rpm, with no light applied and served to test mice´s balance skills in absence of optogenetic stimulation. Only mice able to pass the "*Pre Test*" were tested on the next day. The "*Test Day"* was performed throughout 4 trials at a fixed speed of 16 rpm, with OFF trials (no photostimulation) alternated with ON trials (photostimulation). The laser was started 5 s after the mouse was placed on the rod, in conjunction with the start of each ON trial, and turned off when the animal fell or when the 120s time slice was over. Latency to fall was automatically scored by the Ethovision XT13.0 tracking software (Noldus Information Technology, The Netherlands). When more than one attempt was needed, or when an animal was not able to stay on the rod for 120 s, only the best performance among the 3 attempts was taken for statistical analysis.

Beam Walk Test

Mice were trained to walk from a start position along a wooden round beam (80 cm of total length, 25, 21 and 15 mm diameter) to a goal cage. The beams were placed horizontally, elevated 40 cm from the bench, with one end held by a metal holder and the other one leaned against a neutral cage. The whole beam was divided in 3 parts: a "Starting Area" (SA, 10 cm length) which was brightly lit with a 60 W lamp to induce an aversive stimulus to move forward on the beam, a "Recording Area" (RA, 60 cm segment) where all the parameters were assessed, and a "Goal Zone" (GZ, 10 cm) attached to a cage (clean bedding and home cage nesting material) into which the mouse could escape. On the "*Training Days*" (TD) trials were performed on the 25, 21 (TD 1) and 15 mm (TD 2) diameter beams until two consecutive trials were performed with no stopping. Mice were individually placed in the goal cage for 15 min before starting the training in order to recover from optic cable connection and habituate to the goal cage. Subsequently mice were individually positioned on the SA and allowed to walk to the GZ. On the "*Test*" day, four different conditions were tested on a 15 mm diameter beam. Latency to cross the RA and number of hind foot slips were recorded and scored according to the pre-defined rating scale (Table after [1] and adapted for mice). The software EthoVision XT 13 was used to record the time to cross the RA, while the

number of hind foot slips were recorded manually. Each trial session was started by the mouse entering the RA and ended by the mouse reaching the GZ or falling from the beam. Resting time in the goal cage lasted for 3 min between sessions. The four tested condition were: "*Baseline*" (BS), to measure mice balance skills in absence of photostimulation; "*Alternated Light*" (ALT), with photostimulation applied in alternated 15 cm-segments within the RA (OFF and ON sectors); "*Continuous Light*" (CONT), with the photostimulation applied across the whole RA, turned on by the mouse entering the RA and turned off by reaching the GZ or falling from the beam; "Prior Stimulation" (PRIOR), with the photostimulation delivered from 15 s before positioning the mouse on the SA of the beam until the GZ was reached or the mouse fell. For each condition two trials in which the mouse did not stall on the beam were averaged. The pre-defined rating scale "Neuroscore" was designed by having the maximum score set to 10 points for each condition (1-5 points for latency to cross + 1-5 points for hind-foot slips). The lower the score, the better was the motor performance. See Supplementary Table 1 for scoring scale.

Statistics

Results from all statistical analyses are shown in Supplementary Table 1. Data from behavioral test are expressed on the plots as means ± SEM and when necessary were averaged for the two ON and OFF trials. For statistical analysis Two tailed Wilcoxon matched-pairs test or RM Two-way ANOVA were performed followed by Bonferroni's or Tukey's multiple comparisons where appropriate.

Normal distribution of residuals was checked by using QQ plot and Shapiro-Wilk W test. Rank based z score transformation was applied prior the Two-way ANOVA analysis when more than two outliers were detected. For single cell extracellular recordings Friedman test was performed followed by Dunn's multiple comparisons. For rotarod test and beam walk test, Friedman test was performed followed by Dunn's multiple comparisons (GraphPad Prism version 7.00 for Windows, GraphPad Software, La Jolla California USA).

1. Korenova M, Zilka N, Stozicka Z, Bugos O, Vanicky I, Novak M. NeuroScale, the battery of behavioral tests with novel scoring system for phenotyping of transgenic rat model of tauopathy. *J Neurosci Methods*. 2009;177(1):108-114. doi:10.1016/j.jneumeth.2008.09.027

Supplementary table 1

Figure		Description	N-Number	Statistic	P-value	Post-hoc	Post-hoc P-value
1	A	Schematic representation from virus injections to laser stimulation					
	B, C, D, E, F, G	Histology: Representative injection site and projecting areas					
	H, H'	C-Fos Pitx2/ChR2-eYFP + light stimulation					
	I, I'	C-Fos Pitx2/ChR2-eYFP no light stimulation					
	J, J'	C-Fos Pitx2-Cre-Pitx2/eYFP + light stimulation					
2	A	Schematic representation of the procedure (STN optotagging)					
	B	STN optotagging, representative PSTH					
	C	Schematic representation of the procedure (GP recordings)					
	D	GP recordings, representative PSTH					
	E	Overlapped recorded spikes from GP neuron	20 neurons, 3 mice				
	F	GP recordings, z-score	12 neurons, 3 mice				
	G	GP recordings, behavioral protocol					
	H	GP recordings, firing rate	12 neurons, 3 mice	Friedman test RM χ2(2)=7	**#p=0.03**	Dunn	***p=0.04**
	I	Histology GP, YFP fibers, pontamine deposit					
	J	Reconstructed mapping of recorded GP neurons					
3	A	OFT, STN photoexcitation, number of rearing	Pitx2/ChR2 17 mice Pitx2/eYFP-C 12 mice	2-way RM ANOVA interaction F(1,27)=27.8	p<0.001	Bonferroni	**Pitx2/ChR2, OFF vs. ON ***p<0.001 Pitx2/ChR2 vs. Pitx2/eYFP-C, ON epoch, *p=0.03**
	B	OFT, STN photoexcitation, distance moved (cm)		2-way RM ANOVA interaction F(1,27)=4.162	p=0.05	Bonferroni	**Pitx2/ChR2, OFF vs. ON *p=0.01**
	C	OFT, STN photoexcitation, speed (cm/s)		2-way RM ANOVA interaction F(1,27)=4.307	p=0.05	Bonferroni	**Pitx2/ChR2, OFF vs. ON *p=0.01**
	D	OFT, STN photoexcitation, time spent moving (s)		2-way RM ANOVA stimulation F(1,27)=4.345 interaction F(1,27)=7.359	p=0.05 p=0.01	Bonferroni	**Pitx2/ChR2, OFF vs. ON, **p=0.002**
	E	OFT, STN photoexcitation, time spent in center (s)		2-way RM ANOVA group F(1,27)=0,06139 stimulation F(1,27)=2,343 interaction F(1,27)=0,8351	P=0,37 P=0,81 p=0.09		
	F	OFT, STN photoexcitation, number of center visits		2-way RM ANOVA group F(1,27)=0.05901 stimulation F(1,27)=2.87 interaction F(1,27)=3.121	p=0.81 p=0.10 p=0.09	Bonferroni	**Pitx2/ChR2, OFF vs. ON *p=0.02**
	G	OFT, STN photoexcitation, grooming (s)		2-way RM ANOVA group F(1,27)=39.33 stimulation F(1,27)=38.73 interaction F(1,27)=47.39	p<0.001 p<0.001 p<0.001	Bonferroni	**Pitx2/ChR2, OFF vs ON, ***p<0.001 Pitx2/ChR2 vs Pitx/eYFP-C, ON epoch, ***p<0.001**
	H	OFT, STN photoexcitation, number of jumps		Two-tailed Wilcoxon matched-pairs test	**Pitx2/ChR2 OFF vs. ON, *p=0.02**		
	I	OFT, STN photoinhibition, number of rearing	Pitx2/Arch 20 mice Pitx2/eYFP-A 12 mice	2-way RM ANOVA group F(1,30)=1.348 stimulation F(1,30)=31.02 interaction F(1,30)=32.92	p=0.25 p<0.001 p<0.001	Bonferroni	**Pitx/Arch, OFF vs. ON, ***p<0.001 Pitx2/Arch vs Pitx2/eYFP-A, ON epoch, **p=0.08**
	J	OFT, STN photoinhibition, distance moved (cm)		2-way RM ANOVA group F(1,30)=0.3545 stimulation F(1,30)=21.93 interaction F(1,30)=15	p=0.56 p<0.001 p<0.001	Bonferroni	**Pitx2/Arch vs. Pitx2/eYFP-A, ON epoch, ***p<0.001 Pitx2/Arch vs.Pitx2/eYFP-A, ON epoch, *p=0.03**
	K	OFT, STN photoinhibition, speed (cm/s)		2-way RM ANOVA group F(1,30)=0.3567 stimulation F(1,30)=22 interaction F(1,30)=14.85	p=0.55 p<0.001 p<0.001	Bonferroni	**Pitx2/Arch, OFF vs. ON, ***p<0.001 Pitx2/Arch vs. Pitx2/eYFP-A, ON epoch, *p=0.04**
	L	OFT, STN photoinhibition, time spent moving (s)		2-way RM ANOVA group F(1,30)=0.06385 stimulation F(1,30)=30.02 interaction F(1,30)=25.38	p=0.80 p<0.001 p<0.001	Bonferroni	**Pitx2/Arch, OFF vs. ON, ***p<0.001 Pitx2/Arch vs.Pitx2/eYFP-A, ON epoch, *p=0.04**
	M	OFT, STN photoinhibition,time spent in the center (s)		2-way RM ANOVA group F(1,30)=0,6913 stimulation F(1,30)=3,051 interaction F(1,30)=0,734	p=0.41 p=0.09 p=0.40		
	N	OFT, STN photoinhibition, number of center visits		2-way RM ANOVA group F(1,30)=0.2227 stimulation F(1,30)=3.839 interaction F(1,30)=2.54	p=0.64 p=0.06 p=0.12	Bonferroni	**Pitx2/Arch OFF vs. ON, *p=0.01**
	O	OFT, STN photoinhibition, grooming (s)		2-way RM ANOVA group F(1,30)=0.1859 stimulation F(1,30)=4.358 interaction F(1,30)=0.7507	p=0.67 p=0.05 p=0.39	Bonferroni	**Pitx2/Arch, OFF vs. ON, *p=0.04**
4	A	OFT unilateral stim, experimental setup					
	B	OFT unilateral stim, STN photoexcitation, illustration ipsilateral rotations					
	C	OFT unilateral stim, STN photoexcitation, number of rotations	Pitx2/ChR2 17 mice	2-way RM ANOVA stimulation F(3,39)= 40.08 rotation side F(1,13)=129.8 interaction F(3,39)=49.58	p<0.001 p<0.001 p<0.001	Tukey	**Ipsilateral vs. contralateral, ON1 epoch, ***p<0.001 Ipsilateral vs. contralateral, ON2 epoch, ***p<0.001 Ipsilateral rotations ON1 vs OFF1, ***p<0.001 Ipsilateral rotations ON1 vs OFF2, ***p<0.001 Ipsilateral rotations ON2 vs OFF1, ***p<0.001 Ipsilateral rotations ON2 vs OFF2, ***p<0.001**
	D	OFT unilateral stim, STN photoexcitation, number of rotations, Pitx2/eYFP-C	Pitx2/eYFP-C 12 mice	2-way RM ANOVA stimulation F(3,60)=2.255 rotation side F(1,20)=0.08884 interaction F(3,60)=1.545	p=0.09 p=0.77 p=0.21		
	E	OFT unilateral stim, STN photoinhibition, illustration contralateral rotations					
	F	OFT unilateral stim, STN photoinhibition, number of rotations	Pitx2/Arch 14 mice	2-way RM ANOVA stimulation F(3,39)=10.04 rotation side F(1,13)=35.21 interaction F(3,39)=4.189	p<0.001 p<0.001 p=0.01	Tukey	**Ipsilateral vs. contralateral, ON1 epoch **p=0.001 Ipsilateral vs. contralateral, ON2 epoch **p<0.01 Contralateral rotations ON1 vs OFF1, *p=0.03 Contralateral rotations ON1 vs OFF2, **p=0.005 Contralateral rotations ON2 vs OFF1, *p=0.03 Contralateral rotations ON2 vs OFF2, **p=0.006**
	G	OFT unilateral stim, STN photoinhibition, number of rotations, Pitx2/eYFP-A	Pitx2/eYFP-A 5 mice	2-way RM ANOVA stimulation F(3,12)=1.197 rotation side F(1,4)=0.7826 interaction F(3,12)=4.222	p=0.35 p=0.43 p=0.03	Tukey	no differences
	H	OFT unilateral stim, STN photoexcitation, distance moved (cm)	Pitx2/ChR2 17 mice Pitx2/eYFP-C 12 mice	2-way RM ANOVA group F(1,23) = 7.438 stimulation F(1, 23) = 4.953 interaction F(1, 23) = 8.637	p=0.01 p=0.04 p=0.007	Bonferroni	**Pitx2/ChR2, ON vs. OFF, **p=0.001 Pitx2/ChR2 vs. Pitx2/YFP-C, ***p<0.001**
	I	OFT unilateral stim, STN photoexcitation, speed (cm/s)		2-way RM ANOVA group F(1, 23) = 8.496 stimulation F(1, 23) = 6.822 interaction F(1, 23) = 11.34	p=0.008 p=0.02 p=0.003	Bonferroni	**Pitx2/ChR2, ON vs. OFF, ***p<0.001 Pitx2/ChR2 vs. Pitx2/YFP-C, ***p<0.001**
	J	OFT unilateral stim, STN photoexcitation, number of rearing		2-way RM ANOVA group F(1,23)=0.2287 stimulation F(1,23)=0.4001 interaction F(1,23)=8.631	p=0.64 p=0.53 p=0.007	Bonferroni	**Pitx2/ChR2, ON vs. OFF, *p=0.026**
	K	OFT unilateral stim, STN photoexcitation, grooming (s)		2-way RM ANOVA group F(1,23) = 0.2106 stimulatin F(1,23) = 0.06345 interaction F(1, 23) = 4.815	p=0.65 p=0.80 p=0.04	Bonferroni	no differences
	L	OFT unilateral stim, STN photoinhibition, distance moved (cm)	Pitx2/Arch 14 mice Pitx2/eYFP-A 5 mice	2-way RM ANOVA group F(1,17) = 3.091 stimulation F(1, 17) = 4.25 interaction F(1, 17) = 5.667	p=0.10 p=0.05 p=0.03	Bonferroni	**Pitx2/Arch, OFF vs. ON, ***p<0.001 Pitx2/Arch vs.Pitx2/eYFP-A, ON epoch, *p=0.04**
	M	OFT unilateral stim, STN photoinhibition, speed (cm/s)		2-way RM ANOVA group F(1,17) = 3.08 stimulation F(1, 17) = 4.072 interaction F(1, 17) = 5.504	p=0.10 p=0.06 p=0.03	Bonferroni	**Pitx2/Arch, OFF vs. ON, **p=0.001 Pitx2/Arch vs. Pitx2/eYFP-A, ON epoch, *p=0.04**
	N	OFT unilateral stim, STN photoinhibition, number of rearing		2-way RM ANOVA group F(1,17) = 3.614 stimulation F(1, 17) = 26.17 interaction F(1, 17) = 4.771	p=0.07 p<0.001 p=0.04	Bonferroni	**Pitx2/Arch, OFF vs. ON, ***p<0.001 Pitx2/Arch vs.Pitx2/eYFP-A, ON epoch, *p=0.04**
	O	OFT unilateral stim, STN photoinhibition, grooming (s)		2-way RM ANOVA group F(1,17) = 0.1955 stimulation F(1, 17) = 7.939 interaction F(1, 17) = 1.312	p=0.66 p=0.01 p=0.27	Bonferroni	no differences
5	A	Rotarod, experimental setup					
	B	Rotarod, illustration of the setup					
	C	Rotarod, STN photoexcitation, Pitx2/ChR2, latency to fall (s)	Pitx2/ChR2 17 mice	Friedman test RM χ2(3)= 28.46	p<0.001	Dunn	**OFF 1 vs. ON 1, ***p<0.001 OFF 1 vs. ON 2, **p=0.004 ON 1 vs. OFF 2, ***p<0.001 OFF 2 vs. ON 2, **p<0.004**
	D	Rotarod, STN photoexcitation, Pitx2/eYFP-C, latency to fall (s)	Pitx2/eYFP-C 12 mice	Friedman test χ2(3)=4,655	p=0.1989		
	E	BWT, experimental setup					
	F	BWT, illustration of the different conditions					
	G	BWT, STN photoexcitation, Pitx2/ChR2, Neuroscore	Pitx2/ChR2 17 mice	Friedman test RM χ2(3)= 16.24	p<0.001	Dunn	**BS vs. Prior, **p=0.007 ALT vs. PRIOR, **p=0.005 CONT vs. PRIOR, *p=0.03**
	H	BWT, STN photoexcitation, Pitx2/eYFP-C, Neuroscore	Pitx2/eYFP-C 12 mice	Friedman test χ2(3)=8.895	p=0.03	Dunn	no differences
S1	A	OFT unilateral stim, STN photoexcitation, Pitx2/ChR2, number of jumps	Pitx2/eYFP-C 12 mice	Two-tailed Wilcoxon matched-pairs test	**ON vs. OFF, **p=0.008**		

SCORING SCALE

Latency to cross– (normal 0; maximum 5)
0 Latency ≤ 3 s
1 Latency >3 and ≤ 5 s
2 Latency >5 and ≤ 7 s
3 Latency >7 and ≤ 9 s
4 Latency >9 and ≤ 11
5 Latency > 11 s; animal is not able to perform the task or fall

Hind-foot slips – (normal 0; maximum 5)
0 Hind-foot slips ≤ 1
1 Hind-foot slips >1 and ≤ 2
2 Hind-foot slips >2 and ≤ 3
3 Hind-foot slips >3 and ≤ 5
4 Hind-foot slips >5 and ≤ 8
5 Hind-foot slips >8; animal is not able to perform the task or fall